

The Effect of Pyrimidine Bases on the Hole-Transfer Coupling in DNA<sup>†</sup>Janusz Rak,<sup>\*,§</sup> Alexander A. Voityuk,<sup>‡</sup> Antonio Marquez,<sup>||</sup> and Notker Rösch<sup>\*,‡</sup>

*Institut für Physikalische und Theoretische Chemie, Technische Universität München, 85747 Garching, Germany, Department of Chemistry, University of Gdańsk, Sobieskiego 18, 80–353 Gdańsk, Poland, and Departamento de Química Física, Facultad de Química, Universidad de Sevilla, CL/Prof. García González s/n, 41012-Sevilla, Spain*

*Received: November 30, 2001; In Final Form: April 25, 2002*

Electron hole migration along the  $\pi$ -stack of DNA is mediated by the electronic coupling between the purines (guanine, adenine) of adjacent Watson–Crick pairs (WCPs). We have investigated the effect of the complementary pyrimidines (cytosine, thymine) on this coupling using the two-state model of electron transfer where, at the Hartree–Fock level, the hole-transfer coupling can be described by the energy splitting of the HOMO and HOMO-1 molecular orbitals of WCP dimers. Using the constrained space orbital variation method, we considered the effects of exchange, polarization, and electrostatic interactions (including hydrogen bonds of a WCP) of pyrimidines on the purine–purine electronic couplings. We also performed a detailed analysis of HOMO and HOMO-1 of the duplexes. We conclude that the effect of pyrimidines on the electronic coupling of neighboring purines cannot be described via perturbation theory nor simply reduced to an electrostatic polarization of the purines. However, the combination of exchange (frozen core) and electrostatic effects reproduces the coupling matrix elements between adjacent WCPs rather well. Analysis of the spatial overlap between orbital fragments of HOMO and HOMO-1 suggests that hydrogen bonds between complementary bases play a crucial role in the electronic coupling of neighboring WCPs.

## Introduction

Charge migration in DNA is a rapidly developing area that attracts both experimentalists<sup>1–5</sup> and theoreticians.<sup>6–8</sup> Most of these studies are devoted to the transfer of positive charge (electron holes). Electron transfer through the  $\pi$ -stack of DNA has practical as well as fundamental aspects. Charge transfer in DNA is important for elucidating the long-distance oxidative damage and/or mutations of DNA<sup>9,10</sup> as well as for its potential application in nanoelectronics<sup>11,12</sup> and biosensoric devices.<sup>13</sup> Such studies also contribute to our basic understanding of the differences between electron transfer in DNA and in proteins.<sup>14</sup>

Currently, hole migration in DNA is discussed as a long-range multistep hopping process between sites of similar energetics which are able to localize charge temporarily or permanently.<sup>15–19</sup> The individual short-range hopping events are described as superexchange-mediated tunneling steps between guanine (G) sites, separated by Watson–Crick pairs (WCP) of adenine (A) and thymine (T).<sup>16,19</sup> G sites are energetically preferred.<sup>20,21</sup> Calculations in model duplexes 5'-XBY-3' demonstrated<sup>22</sup> that the energy for hole transfer between cation radical states B<sup>+</sup> of a nucleobase are considerably influenced by the subsequent base Y while the effect of the preceding base X is rather small. In similar environment, a localized cationic state of guanine is calculated to be more stable than that localized on adenine, thymine, and cytosine (C) by 0.44, 1.28, and 1.55 eV, respectively.<sup>22</sup> Thus, normally only off-resonance coupling between G<sup>+</sup> and other nucleobase cation radicals can take place.

The rate constant  $k_{\text{DA}}$  of the nonadiabatic charge transfer from a donor D to an acceptor A is determined by the effective electronic coupling  $H_{\text{DA}}$  and the thermally weighted Franck–Condon Factor (FC)<sup>6,23,24</sup>

$$k_{\text{DA}} = \frac{2\pi}{\hbar} H_{\text{DA}}^2 (\text{FC}) \quad (1)$$

The electronic coupling  $H_{\text{DA}}$  can be calculated by using an effective Hamiltonian<sup>25,26</sup> with diagonal elements determined by ionization energies of nucleobases and off-diagonal elements equal to the corresponding electronic coupling  $V$  of neighboring nucleobases (or WCPs).<sup>27,28</sup> It has been demonstrated that the electronic coupling between adjacent WCPs is very sensitive to the conformation of the dimer duplexes.<sup>29</sup> Moreover, chemical modification of nucleobases can significantly influence the charge-transfer efficiency.<sup>28,30,31</sup>

Because the purine bases G and A exhibit lower ionization potentials than the pyrimidine bases C and T, it is meaningful to discuss preferentially the electronic coupling between such neighboring units as resting or intermediate sites of a superexchange-based description of charge migration in DNA.<sup>32,33</sup> Pyrimidine bases exert a significant influence on the coupling between the purine bases. This is clearly demonstrated by comparing the coupling matrix elements  $V$  calculated for models which contain purines moieties only to couplings determined for systems that comprise complete dimer duplexes, i.e., the corresponding WCP dimers (Figure 1).<sup>33</sup> This effect of the pyrimidine bases on the electronic coupling between adjacent purine moieties was analyzed<sup>33</sup> by invoking the concept of interfering transfer pathways.<sup>26</sup> If one estimates the contributions of these additional transfer pathways by perturbation theory, one brings the superexchange concept to bear *within* a WCP dimer, with the pyrimidine units acting as bridge sites.<sup>33</sup>

<sup>†</sup> Dedicated to Professor Roald Hoffmann on the occasion of his 65th birthday.

<sup>\*</sup> To whom correspondence should be addressed.

<sup>‡</sup> Institut für Physikalische und Theoretische Chemie.

<sup>§</sup> Department of Chemistry.

<sup>||</sup> Departamento de Química Física.

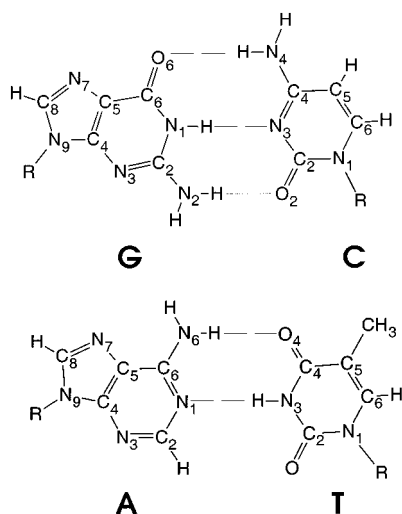


**Figure 1.** Schematic representation of the Watson–Crick pairs (GC) and (AT).

However, the perturbation based rationalization was not fully satisfactory because the resulting corrections to the electronic coupling between the isolated purines turned out too small.<sup>33</sup> Therefore, other interaction mechanisms have to be at work within WCPs; recall the dipolar character of the charge distribution of pyrimidines and the hydrogen bonds between complementary nucleobases. To clarify the role of the pyrimidine units, a more comprehensive analysis of the electronic coupling for hole transfer between adjacent base pairs is desirable.

In the following we will present several arguments supporting the view that pyrimidine bases affect the hole transfer in DNA mainly through electrostatic, exchange, and polarization interactions with purine bases. We will rely on the two-state model of electron transfer where, at the Hartree–Fock level, the hole-transfer coupling can be described by the energy splitting of the HOMO and HOMO-1 molecular orbitals of WCP dimers.<sup>6,34</sup> First, we will analyze these pertinent molecular orbitals when the electronic states of the hole donor and acceptor are “in resonance”. Next, we will investigate electrostatic and polarization effects by replacing the pyrimidine units with atomic point charge models. For a systematic and quantitative assessment of the effects of the pyrimidines on the electronic coupling between neighboring purines in DNA, we will apply the constrained space orbital variation method (CSOV) which has been successfully employed for analyzing metal–ligand bonding in complexes and adsorbate–substrate interactions.<sup>35–37</sup> Finally, we will inspect the spatial characteristics of the HOMO and HOMO-1 orbitals to promote a qualitative understanding of the electronic coupling variation.

## Methods

We consider the stacked nucleobases as mediators of the hole transfer in DNA. Based on previous results<sup>27</sup> it is justified to neglect the effect of the sugar–phosphate backbone. Ten possible WCP dimers of regular structure were examined. Their geometries were generated with the program SCHNARP,<sup>38</sup> using the step parameters rise = 3.38 Å and twist = 36°. Abbreviated notations are employed to identify the dimers; for instance, [(TA),(GC)] or TG designates a complex that consists of the two Watson–Crick pairs (TA) and (GC) in the order 5′ → 3′.<sup>33</sup>

The electronic coupling matrix elements  $V$  for hole transfer were estimated within the two-state model of electron transfer.<sup>6</sup> For dimers with equivalent hole donors and acceptors, i.e.,

**TABLE 1:** Effect of an External Electric Field  $F$  on the Hole Coupling Matrix Element  $H_{DA}$  between WCPs of the Dimer [(GC), (AT)] Calculated at The HF/6-31G\* Level with the GMH Scheme, and Also Given Is the Energy Splitting  $\Delta$  between the Adiabatic States

| $F$ [ $10^{-4}$ au] | $\Delta$ [eV]      | $H_{DA}$ [eV] |
|---------------------|--------------------|---------------|
| 80                  | 0.557              | 0.1267        |
| 40                  | 0.998              | 0.1267        |
| 0                   | 0.467              | 0.1271        |
| −27                 | 0.255 <sup>a</sup> | 0.1274        |
| −40                 | 0.315              | 0.1276        |
| −90                 | 0.941              | 0.1283        |
| −130                | 1.501              | 0.1293        |

<sup>a</sup> Minimum energy splitting.

[(GC),(CG)], [(CG),(GC)], [(AT),(TA)], and [(TA),(AT)],  $V$  is taken as the half of the energy splitting  $\Delta = E_2 - E_1$  of the adiabatic states of the cationic system, e.g. [(G<sup>+</sup>C),(CG)] and [(GC),(CG<sup>+</sup>)]. In the remaining WCP dimers, donor and acceptor are not equivalent; therefore, the minimum splitting between the two adiabatic states has to be found. For this purpose an external electric field was applied along the DNA axis, to bring donor and acceptor states into resonance.<sup>33,39</sup> Invoking Koopmans’ theorem, the energy splitting  $\Delta$  can be approximated as the difference of the one-electron energies of the HOMO (highest occupied molecular orbital) and the adjacent lower-lying HOMO-1 orbital of the corresponding closed-shell neutral species,  $\Delta = \epsilon_{\text{HOMO}-1} - \epsilon_{\text{HOMO}}$ . It has been shown that this Hartree–Fock (HF) based approach yields results in close agreement with those of a more accurate treatment including electron correlation.<sup>34</sup> Note that Koopmans’ approximation suppresses ionization-induced relaxation effects within a fragment. However, these effects will essentially cancel if one compares the resulting electronic couplings between  $\pi$ -stacked purines and the corresponding WCP dimers. Advantages and limitations of applying Koopmans’ theorem to calculate the electronic coupling have been discussed in detail elsewhere; see refs 6 and 27 and reference therein.

As already mentioned, a weak external electric field is used to bring donor and acceptor levels into resonance. Since the electric field was applied in the direction parallel to the DNA axis (i.e., perpendicular to the planes of the nucleobase),  $\pi$ -type MOs of remain practically unchanged by the perturbation and, therefore, there is no essential polarization artifact of HOMO and HOMO-1. To corroborate that matrix elements  $V$  obtained with the above procedure are essentially independent of the electric field, we calculated  $V$  for the duplex dimer [(GC),(AT)], for example, with the generalized Mulliken-Hush method (GMH).<sup>40,41</sup> That method is applicable *without and with* external electric field. In the two-state model used here, the GMH-based electronic coupling can be expressed by the adiabatic splitting  $\Delta$ , the difference between the dipole moments  $\mu_1 - \mu_2$  of those states, and finally, the corresponding transition dipole moment  $\mu_{12}$ .<sup>40,41</sup>

$$H_{DA} = \frac{\Delta |\mu_{12}|}{\sqrt{(\mu_1 - \mu_2)^2 + 4\mu_{12}^2}} \quad (2)$$

Note that variation of the electric field strength significantly modifies the energy gap between the adiabatic states, but leaves the electronic coupling almost unchanged (Table 1), even for relatively strong electric fields  $F$  of  $8 \times 10^{-3}$  and  $-13 \times 10^{-3}$  au. Deviations from the value at the “resonance” field  $2.7 \times 10^{-3}$  au amount to −0.5 and 1.5%, respectively (Table 1). The coupling values obtained for the WCP dimer [(GC),(AT)] with

**TABLE 2: Electronic Coupling Matrix Elements  $V$  for Hole Transfer for All Ten Purine Donor–Acceptor Systems Possible in DNA<sup>a</sup>**

| WCP dimer   | $V$                               |  |                    |           | $\Delta V$ , CSOV |         |                     |         |                     |        |
|-------------|-----------------------------------|--|--------------------|-----------|-------------------|---------|---------------------|---------|---------------------|--------|
|             | pu <sub>1</sub> :pu <sub>2a</sub> | pu <sub>1</sub> :pu <sub>2</sub> , ESP | dimer <sup>b</sup> | dimer, fc | fc                | pu pol. | pu $\rightarrow$ py | py pol. | py $\rightarrow$ pu | SCF    |
| [(GC),(GC)] | 0.084                             | 0.089                                  | 0.093              | 0.096     | 3%                | −0.006  | 0.000               | 0.004   | 0.001               | −0.002 |
| [(AT),(AT)] | 0.030                             | 0.028                                  | 0.026              | 0.025     | 4%                | 0.002   | 0.000               | −0.001  | −0.001              | 0.001  |
| [(GC),(AT)] | 0.089                             | 0.109                                  | 0.122              | 0.116     | −5%               | −0.005  | 0.002               | 0.008   | 0.002               | −0.001 |
| [(AT),(GC)] | 0.049                             | 0.033                                  | 0.025              | 0.030     | 20%               | 0.002   | −0.002              | −0.004  | −0.001              | 0.000  |
| [(GC),(CG)] | 0.019                             | 0.020                                  | 0.022              | 0.022     | 0%                | −0.001  | 0.001               | −0.001  | 0.000               | 0.001  |
| [(CG),(GC)] | 0.043                             | 0.060                                  | 0.079              | 0.072     | −9%               | −0.008  | 0.001               | 0.009   | 0.003               | 0.002  |
| [(AT),(TA)] | 0.034                             | 0.045                                  | 0.055              | 0.055     | 0%                | −0.004  | 0.001               | 0.003   | 0.003               | −0.003 |
| [(TA),(AT)] | 0.062                             | 0.066                                  | 0.050              | 0.061     | 22%               | −0.002  | −0.001              | 0.000   | 0.000               | −0.007 |
| [(GC),(TA)] | 0.021                             | 0.019                                  | 0.026              | 0.026     | 0%                | 0.000   | 0.001               | −0.002  | 0.001               | 0.000  |
| [(TA),(GC)] | 0.004                             | 0.013                                  | 0.027              | 0.019     | 30%               | −0.001  | 0.002               | 0.005   | 0.000               | 0.002  |

<sup>a</sup> Comparison of results for systems which consist of the purine nucleobases only (pu<sub>1</sub>:pu<sub>2</sub>) and of these purine in the electrostatic field of the corresponding pyrimidines described by ESP point charges (pu<sub>1</sub>:pu<sub>2</sub>, ESP), to those for the complete WCP dimers as well as the WCP dimer treated in the first, “frozen core” step of the CSOV analysis (dimer, fc). The results of the remaining CSOV steps are indicated as increments  $\Delta V$  relative to the preceding CSOV step (see text): (ii) polarization of the purine moieties (pu pol.), (iii) charge transfer from the purine to the pyrimidine units (pu  $\rightarrow$  py), (iv) polarization of the pyrimidine units (py pol.), (v) back transfer from the pyrimidine to the purine units (py  $\rightarrow$  pu), (iv) full SCF treatment of the WCP dimer (SCF). All values in eV. Also shown is the deviation of the frozen core CSOV result of the WCP dimer from the full SCF value (fc, in %). <sup>b</sup> From ref 33.

two rather different approaches (GMH: 0.127 eV, Table 1. “resonance”: 0.122 eV, Table 2.) agree within 4%. These findings strongly corroborate that the “resonance” method in the remainder this work provides reliable electronic coupling values for WCP dimers.

Calculations of electronic coupling matrix elements have been carried out at the HF level employing the standard 6-31G(d) basis set.<sup>42</sup> While for the  $\pi$ -stacked hole donors and acceptors the electron coupling depends crucially on the “tails” of the electronic wave function,<sup>33</sup> this computational procedure was shown to yield sufficiently accurate results.

To model the electrostatic effect of pyrimidine bases in dimers, we employed a set of atomic charges which were fitted at the HF/6-31G(d) level to the electrostatic potential on a set of grid points;<sup>43,44</sup> during the fit, charges were constrained to reproduce the dipole moment of the isolated species T or C.

To analyze polarization effects and exchange repulsion (Pauli repulsion) due to pyrimidine bases in the model duplexes studied, a charge distribution analysis<sup>45</sup> (CDA) of the “resonance” state was carried out. The CDA procedure is based on a representation of the MOs of a compound system A+B in terms of the MOs of the two fragments A and B. In each WCP dimer, we assigned the two purine moieties to fragment A and the two corresponding pyrimidine units to fragment B. The resulting partitioning of an orbital charge distribution and of the total electron density yields (i) electron donation due to the mixing of the occupied orbitals of fragment A with the virtual orbitals of fragment B, (ii) back-donation due to mixing of the occupied orbitals of fragment B with the virtual orbitals of fragment A, and (iii) charge repulsive polarization due to the interaction between the occupied orbitals of both fragments.<sup>45</sup>

For a direct, quantitative assessment of electrostatic, exchange and polarization contributions to the electron coupling matrix element we invoked the CSOV scheme.<sup>35</sup> Again, we take the same two fragments A and B just defined. The CSOV analysis relies on several steps where the orbital space available in the SCF process is increased in stepwise fashion. In each step, the basis comprises the MOs of the preceding step plus additional fragment orbitals as follows. (i) One starts with the “frozen core” step where the MOs of the fragments A and B are mutually orthogonalized, accounting for electrostatic and exchange effects; (ii) then the SCF procedure is restricted to the occupied and virtual space of fragment A while all MOs of fragment B are kept “frozen” (polarization of fragment A); (iii) next, mixing

of the orbitals of fragment A with the virtual orbitals of fragment B is allowed (charge transfer from A to B); steps (iv) and (v) are analogous to steps (ii) and (iii), respectively, but the roles of fragments A and B is reversed; finally, in step (vi) the full orbital relaxation is obtained because all orbitals of both fragments are optimized within the SCF procedure. By calculating the electron coupling matrix element at each CSOV step, one can directly monitor the effect of the various electronic mechanisms. For symmetric systems with equivalent hole donor and acceptor, i.e., [(GC),(CG)], [(CG),(GC)], [(AT),(TA)], and [(TA),(AT)], this analysis has been performed without invoking an external electric field since the electronic states of hole donors and acceptors are in resonance for zero field. In the remaining cases several values of the external electric field have been used, selected specifically for each duplex dimer; at each CSOV step, the HOMO/HOMO-1 energy splitting  $\Delta$  was minimized by interpolating the values resulting for each field. While a CSOV decomposition depends to some extent on the order in which the various terms are extracted, relative changes of these contributions are quite small (several %); this uncertainty is acceptable for our semiquantitative analysis.

For the charge distribution analysis we used the program CDA.<sup>46</sup> The CSOV calculations have been carried out with the help of the HONDO program suite.<sup>47</sup> All other Hartree–Fock SCF calculations were performed with the package Gaussian 98.<sup>48</sup> The MO plots were generated with the program MOLDEN.<sup>49</sup>

## Results and Discussion

**Charge Distribution Analysis and ESP Charge Models.** As mentioned in the Introduction, hole transfer in DNA is mediated by the purines since they exhibit smaller ionization potentials than the pyrimidine moieties. A comparison between the electronic coupling  $V$  calculated for WCP dimers (duplex models) with the results of models which comprise only the purine moieties (pu<sub>1</sub>:pu<sub>2</sub>; see Table 2) clearly demonstrates the significant effect of the pyrimidine units on the hole-transfer coupling between adjacent WCPs.<sup>33</sup> For the pyrimidine bases to act as bridge sites between the purine bases, the HOMO and HOMO-1 of a WCP dimer should exhibit a contribution of the pyrimidine moieties.

Recall that the electronic coupling of donor and acceptor is calculated in the state where the electronic levels of hole donor



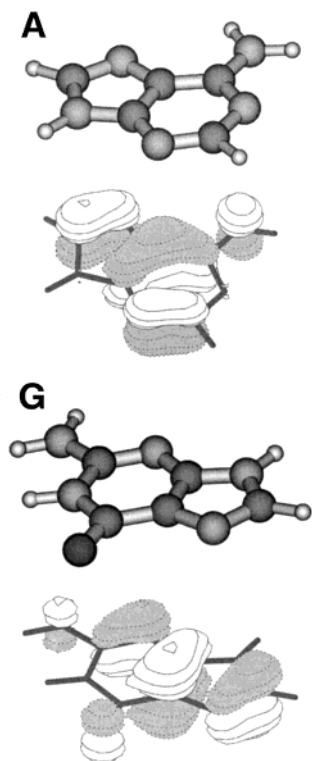


**Figure 2.** Highest occupied molecular orbitals (HOMO) of adenine (A) and guanine (G), plotted for the contour values  $\pm 0.035$  au.

and acceptor are “in resonance”, modeled with the help of an external electric field in the case of an asymmetric WCP dimer. In the absence of an electric field, HOMO and HOMO-1 orbitals of such an asymmetric system are each localized on one or the other purine base. Depending on the localization of the electron hole, the wave function describes one of the two diabatic radical cation states involved in the hole transfer.<sup>34</sup> Figure 2 displays the HOMOs of guanine and adenine; the interaction of these MOs represents the electronic coupling of these two purine nucleobases along the  $\pi$ -stack of DNA.

The two corresponding adiabatic states, which are modeled by applying an external electric field that minimizes the energy splitting of the two hole states,<sup>6,34</sup> are represented by delocalized HOMO and HOMO-1 orbitals. (No further delocalization is observed if more than two WCPs are included in the model.<sup>19,33</sup>) As will be discussed below in more detail, these orbitals are essentially normalized sum or difference of the appropriate HOMO orbitals of the interacting purines. As examples for intra- and interstrand hole-transfer coupling, we show in Figures 3 and 4 the (bonding) HOMO-1 orbitals of the WCP dimers [(GC),(AT)] and [(GC),(TA)], respectively.

To analyze the pertinent wave functions in a quantitative fashion, we applied the CDA procedure to the electronic structure where hole donor and acceptor are in resonance. In Table 3, we collect the resulting electron donation from the purine moieties ( $D$ ), the back-donation ( $B$ ), and the repulsive polarization (RP) for HOMO and HOMO-1 of each WCP dimer in resonance; also listed are the corresponding overall values, calculated as a sum over all occupied MOs. For each HOMO and HOMO-1, the donation  $D$ , characterizing the mixing of pyrimidine MOs into the relevant purine MOs, is very small, at most  $0.006e$  (see [(AT),(TA)] and [(GC,TA)]; Table 3). Note that the back-donation  $B$  vanishes always. The repulsive polarization RP of HOMO and HOMO-1 yields somewhat larger

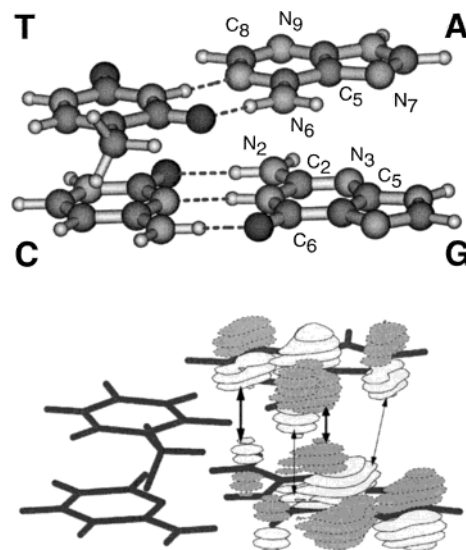


**Figure 3.** Sketch of the HOMO-1 orbital of the WCP dimer [(GC),(AT)] in resonance for hole transfer, an example of intrastrand coupling. The direction 5′–3′ in the upper part is from bottom to top. Arrows indicate overlapping regions between purines orbitals; the width of the arrows provides a rough indication to the magnitude of the overlap. Contour values at  $\pm 0.035$  au.

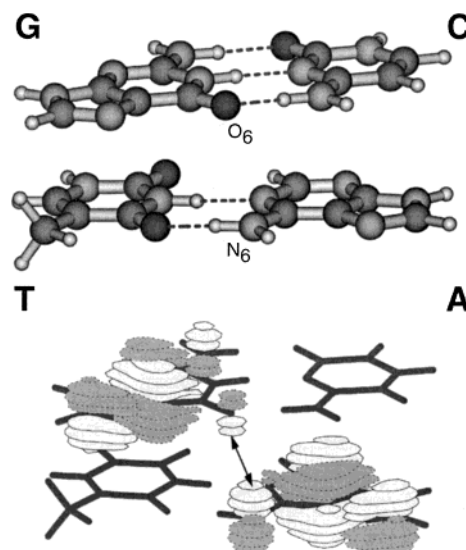


**Figure 4.** Sketch of the HOMO-1 orbital of the WCP dimer [(GC),(TA)] in resonance for hole transfer, an example of interstrand coupling. The direction 5′–3′ in the upper panel is from top to bottom. Layout as in Figure 3.

absolute values than the donation (at most  $0.015$ , see Table 3); the largest values are again observed for [(AT),(TA)] and [(GC,TA)].

The WCP dimers listed in Table 3 can be divided into two groups. The first four duplex systems represent intrastrand hole transfer; the remaining six exhibit interstrand hole transfer. One notices that values of  $D$  and RP of HOMO and HOMO-1, although overall very small, are in general larger for interstrand than those for intrastrand configurations.

These CDA results indicate that HOMO and HOMO-1 do not change qualitatively during the formation of a WCP complex. The last three columns of Table 3 show the corresponding partitions of the overall charge distribution: donation, charge back-donation, and repulsive polarization. Differently from the HOMO and HOMO-1, these overall characteristics, which describe the charge reorganization due to the formation

TABLE 3: CDA Analysis of WCP Dimers in Resonance for Hole Transfer<sup>a</sup>

| WCP dimer   | HOMO  |       |        | HOMO-1 |       |        | total |       |        |
|-------------|-------|-------|--------|--------|-------|--------|-------|-------|--------|
|             | D     | B     | RP     | D      | B     | RP     | D     | B     | RB     |
| [(GC),(GC)] | 0.001 | 0.000 | -0.001 | 0.000  | 0.000 | 0.000  | 0.253 | 0.310 | -0.451 |
| [(AT),(AT)] | 0.000 | 0.000 | -0.001 | 0.000  | 0.000 | -0.001 | 0.205 | 0.220 | -0.375 |
| [(GC),(AT)] | 0.000 | 0.000 | -0.001 | 0.000  | 0.000 | -0.001 | 0.227 | 0.263 | -0.409 |
| [(AT),(GC)] | 0.001 | 0.000 | -0.001 | 0.001  | 0.000 | -0.001 | 0.232 | 0.267 | -0.417 |
| [(GC),(CG)] | 0.003 | 0.000 | -0.012 | 0.004  | 0.000 | -0.009 | 0.270 | 0.362 | -0.512 |
| [(CG),(GC)] | 0.002 | 0.000 | -0.009 | 0.002  | 0.000 | -0.005 | 0.258 | 0.356 | -0.472 |
| [(AT),(TA)] | 0.005 | 0.000 | -0.015 | 0.006  | 0.000 | -0.013 | 0.231 | 0.254 | -0.451 |
| [(TA),(AT)] | 0.003 | 0.000 | -0.003 | 0.003  | 0.000 | -0.010 | 0.219 | 0.255 | -0.402 |
| [(GC),(TA)] | 0.005 | 0.000 | -0.016 | 0.005  | 0.000 | -0.011 | 0.254 | 0.305 | -0.482 |
| [(TA),(GC)] | 0.002 | 0.000 | -0.009 | 0.003  | 0.000 | -0.004 | 0.238 | 0.302 | -0.439 |

<sup>a</sup> Fractions of electron density of the HOMO and HOMO-1 orbitals donated (*D*) from the purine to the pyrimidine moieties and back (*B*) as well as the repulsion polarization (RP) contribution which describes electron density removed from the overlap region of the occupied MOs. Also shown are the corresponding partitions (in *e*) of the total charge density, calculated as the sum over all occupied MOs.

of the complex, admit significant values. The total polarization of the purine fragment is remarkable (Table 3). The largest (absolute) values of the charge redistribution were calculated for the dimer [(GC),(CG)], namely, a donation of 0.270*e* from the purine fragment to pyrimidine fragment and 0.362*e* as back-donation, while 0.512*e* is transferred from the occupied MOs into the nonoverlapping regions (Table 3). The overall electron donation from the purine bases to the pyrimidines is always smaller than the corresponding back-donation. This effect is probably connected to the fact that pyrimidine bases are smaller than purine bases and, therefore, the space of unoccupied MOs of the former is smaller, too.

If one takes all CDA information of Table 3 into account, one is lead to conclude that the influence of the pyrimidine bases on the hole-transfer coupling in DNA is limited to polarization and exchange effects rather than to pyrimidine orbitals being directly involved in the electronic coupling, e.g., via a super-exchange mechanism.

To confirm this hypothesis we have estimated the electronic coupling matrix element *V* for models where pyrimidine units have been replaced by point charges that represent the electrostatic potential of the "missing" nucleobases (ESP model; see the section Methods). The corresponding results are presented in Table 2 under the heading *V*(pu<sub>1</sub>;pu<sub>2</sub>,ESP). For most cases, the ESP model predicts a coupling matrix element close to the arithmetic average of the matrix elements calculated for WCP dimer, *V*(dimer), and the pair of purine bases in the geometry of the WCP dimer, *V*(pu<sub>1</sub>;pu<sub>2</sub>). This estimate fails only for the systems [(TA),(AT)] and [(GC),(TA)] (Table 2). For the dimer [(TA),(AT)] the ESP model slightly overestimates the matrix element as predicted for the two purine bases *V*(pu<sub>1</sub>;pu<sub>2</sub>); for [(GC),(TA)], the ESP model slightly underestimates the coupling (Table 2). Pyrimidine bases are strongly polar; the dipole moments of *T* and *C*, calculated for experimental geometries at the HF/6-31G\* level, are 5.0 and 8.0 D, respectively. If the pyrimidine bases would exert electrostatic and induction effects only, the ESP model would be expected to furnish closer estimates of the matrix elements determined for the WCP dimers.

The most severe limitation of the ESP model is that it lacks exchange repulsion effects due to the occupied MOs of the pyrimidine fragment (two units) in close proximity of the purine fragment (two units). Recall that the CDA analysis indicates very significant repulsive polarization effects in the charge rearrangement as a consequence of the (formal) assembly of the WCP dimer (Table 3). The ESP approach, although very attractive due to its simplicity, is somewhat too simplistic when modeling the hole-transfer coupling in DNA. To overcome the

restrictions of this scheme and to quantify how various interactions mechanisms (electrostatic, exchange and polarization interaction) between purine and pyrimidine units affect the hole-transfer coupling, we will now turn to the results of CSOV analysis.

#### Constrained Space Orbital Variation Analysis (CSOV).

Thus far we have shown that electrostatic and polarization effects alone are not able to account quantitatively for the calculated electronic coupling matrix elements predicted for the WCP dimers. Because of a stepwise increase of the orbital space in HF SCF calculations, a CSOV analysis enables one to monitor how physically meaningful effects related to the interaction between purine and pyrimidine units (i.e. electrostatic, exchange and polarization interaction) affect the electronic coupling. As mentioned above, we employ the same partitioning of a WCP dimer in one fragment of two purine units and the other fragment of the two pyrimidine units as previously used in the CDA analysis. In Table 2 we present an overview of the electronic coupling as determined at each CSOV step; we display the results of the frozen core approximation (sum of electrostatic and exchange interaction) together with increments of the subsequent CSOV steps (intraunit polarization of the purine dimer, charge transfer from the purine to the pyrimidine fragment, intraunit polarization of the pyrimidine dimer, charge transfer from the pyrimidine fragment to the purine fragment, and finally the full SCF approach). In the following discussion of the CSOV results one should keep in mind that the minimization of HOMO and HOMO-1 energy splitting  $\Delta$  as well as rounding errors may introduce uncertainties of about  $\pm 0.001$  eV.

In the majority of cases, the frozen core approximation reproduces the full SCF result within 10%. Note that for the interstrand systems [(GC),(CG)], [(AT),(TA)], and [(GC),(TA)] the agreement is perfect. Only for three dimers, namely [(AT),(GC)], [(TA),(AT)], and [(TA),(GC)], the electronic coupling resulting from the frozen core step overestimates the corresponding full SCF value by 20–30% (Table 2). However, keep in mind that the electronic coupling values *V* of [(AT),(GC)] and [(GC),(TA)] are rather small, 0.025 and 0.027 eV, respectively. Assuming a minimum (absolute) deviation in the frozen core step, this observation rationalizes, at least in part, the large percentage value of the deviation. Note also that for the system [(TA),(AT)], the last CSOV step (full SCF), makes an unusually large contribution (−0.007 eV; Table 2). This finding suggests that polarization effects, not accounted for in frozen core approximation, are relatively important for the WCP dimer [(TA),(AT)].

The frozen core step of the CSOV analysis accounts for the same effects which are reflected by the Heitler–London energy as calculated by symmetry adapted perturbation theory.<sup>50</sup> Thus, the matrix elements calculated in this step are modified, relative to those obtained for isolated purine pairs, by the exchange repulsion caused by the space of occupied MOs of the pyrimidines as well as by electrostatic interactions of the purines with the permanent electric moments of the pyrimidine moieties. Inspection of Table 2 shows that the frozen core approximation reproduces the electronic coupling of WCP dimers very well, much better than the ESP model. Thus, we conclude that not only the electric field generated by the pyrimidine bases affects hole transfer. Rather, pyrimidine-induced exchange effects exert an important influence on the electronic structure of the purine nucleobases.

The remaining CSOV steps describe the effect of the interactions of the fragments, starting from a state restrained by the Pauli principle; one discriminates intraunit (polarization) and interunit (charge transfer) effects. A detailed analysis of Table 2 reveals the rather minor influence of these effects on the matrix elements. For instance, the largest increment due to pyrimidine polarization, 0.009 eV predicted for CC in the complex [(CG),(GC)], accounts only for 11% of the full SCF result. In addition, note that in this system GG polarization contributes  $-0.008$  eV (see Table 2). Therefore the cumulative effect of these two corrections leaves the frozen core value of  $V$  essentially unchanged. This behavior, namely purine and pyrimidine polarization acting in opposite directions, is also observed in most other systems. This is probably connected to the fact that the permanent dipole moment of the first fragment induces a dipole moment contribution of opposite orientation on the second fragment. The systems [(TA),(AT)], [(GC),(TA)], and [(GC),(CG)] provide exceptions. In the first two cases, the polarization of TT or GA, respectively, vanishes. Both polarization contributions vanish almost for the WCP dimer [(GC),(CG)].

The accumulated polarization term essentially vanishes in all cases; the two largest accumulated values are 0.003 and 0.004 eV for [(GC),(AT)] and [(TA),(GC)], respectively (Table 2). The total polarization component added to the frozen core value tends to improve the agreement with the full SCF result (Table 2); in some cases the accumulated polarization contribution has no effect (within rounding errors). Leaving aside the WCP dimer [(TA),(AT)], the largest discrepancy,  $-0.003$  eV, between the full SCF result and the sum of the frozen core and the total polarization effects is observed for the system [(AT),(TA)].

The complex [(TA),(AT)] presents an exception under almost all aspects of our analysis. For this system, the frozen core results deviates significantly (by 22%) from the full SCF result and the electronic coupling determined after the first cycle of the CSOV analysis, i.e., after steps ii–v, deviates by far the most from the full SCF result which is still overestimated by 0.007 eV. This finding is likely related to relatively slow convergence of the CSOV procedure for this complex; further CSOV cycles are expected to remove this discrepancy.<sup>35</sup> In keeping with the findings of the CDA analysis, the CSOV procedure also shows that the increments due to charge transfer are small; the absolute values of the accumulated charge-transfer contributions never exceed 0.004 eV. Strictly speaking, one has to take the effects of the various CSOV steps in their proper order. However, since the individual contributions of the polarization and charge-transfer steps are so small, we may discuss them after regrouping in the spirit of a perturbation argument. In summary, the sum of electrostatic and exchange

effects supplemented with rather minor polarization terms which result from the interaction between purine and pyrimidine units reproduces very well the electron coupling matrix elements calculated for WCP dimers.

**Spatial Characteristics of HOMO and HOMO-1 Orbitals in WCP Dimers.** It is informative to discuss the spatial characteristics of the HOMO and HOMO-1 orbitals and its consequences for the electronic coupling. As examples for this strategy, we shall consider in detail two dimers, [(GC),(AT)] and [(GC),(TA)], for intrastrand and interstrand coupling, respectively. For both examples chosen, inclusion of the complementary pyrimidine bases increases the electronic coupling relative to the simple model which consists of the corresponding pair of purines only (see Table 2).

The magnitude of the electronic coupling  $V$  between a donor  $D$  and an acceptor  $A$  depends on the overlap between  $\Psi_D$  and  $\Psi_A$  wave functions ( $V \langle \Psi_D | \Psi_A \rangle$ ) and hence on the electron density in the overlap region. Therefore, a topological analysis of overlap between the HOMO of the purines in HOMO or HOMO-1 orbitals of a WCP should provide qualitative information related to the influence of the pyrimidine nucleobases on the calculated coupling.

Recall that the HOMO of an asymmetric duplex is localized on one of the purine bases while the HOMO-1 orbital is localized on the adjacent purine basis. Within the framework of the two-state model, the corresponding electron hole states represent the diabatic states involved in hole transfer.<sup>34</sup> Figure 2 displays the HOMOs of adenine and guanine. The HOMO and HOMO-1 orbitals of a WCP dimer “in resonance” complexes are the antibonding and bonding combinations, respectively, of the HOMO orbitals of the two purines (see Figures 3 and 4).

Thus, for the intrastrand example [(GC),(AT)] the leading orbital overlap is related to the interaction of  $N_2$  and  $N_3$  of guanine with the centers  $C_8$  and  $C_5$  of adenine (see Figure 3). There are also minor interactions between the centers  $C_6$  and  $C_5$  of guanine and the centers  $N_6$  and  $N_7$  of adenine. These overlap regions should be responsible for the electronic coupling. Note that two overlapping regions (major  $N_2-C_8$ , minor  $C_6-N_6$ ; see Figure 3) involve the amino groups of the purines, thus point to the *hydrogen bonds* formed with complementary pyrimidine bases:  $N_2H \cdots O_2$  in (GC) and  $N_6H \cdots O_4$  in (AT) (Figure 1). With the formation of a hydrogen bond, the electron density increases at the proton-donor group and simultaneously decreases at the proton-acceptor center.<sup>51</sup> The overlapping regions of interest involve the proton donors  $N_2$  of G and  $N_6$  of A. Therefore, the electron density at these atoms should increase when hydrogen bonds between purines and pyrimidines are formed. As a result, in the WCP dimer [(GC),(AT)] we expected a larger contribution of the  $p_\pi$  atomic orbitals of  $N_2$  and  $N_6$ , as compared with the simple model  $pu_1:pu_2$ . In the spirit of the discussion above, this should translate into an increased overlap between hole donor and hole acceptor, and therefore to a larger electronic coupling  $V$ . Changes in the LCAO coefficients of the HOMO and HOMO-1 orbitals directly lead to a modification of the electron coupling matrix elements since our models do not involve any geometry changes.

In Table 4 we display the LCAO coefficients of the “contact” centers identified above for the HOMO-1 of [(GC),(AT)]. As can be seen, the LCAO coefficients for both proton donors,  $N_2$  of G and  $N_6$  of A, increase when the pyrimidines are included. The effect is more pronounced for the contact  $N_2-C_8$  than for  $N_6-C_6$ . These increased values of the LCAO coefficients



**TABLE 4: Effect of the Hydrogen Bonds within a WCP on the Electron Coupling between Selected Neighboring Purines Demonstrated by Comparing the Composition of the HOMO-1 Orbitals of Systems, Characterized by the Coefficients of p Atomic Orbitals Associated with Atomic Centers that Are Involved in Hydrogen Bonds: Comparison of Systems that Consist of Neighboring Purines Only (G:A) and the Corresponding WCP Dimers**

| system      | atomic center <sup>a</sup> | first set <sup>b</sup> |           | second set <sup>b</sup> |           |
|-------------|----------------------------|------------------------|-----------|-------------------------|-----------|
|             |                            | G:A                    | WCP dimer | G:A                     | WCP dimer |
| [(GC),(AT)] | N <sub>2</sub> (G)         | 0.085                  | 0.113     | 0.102                   | 0.126     |
|             | N <sub>6</sub> (A)         | -0.174                 | -0.176    | -0.179                  | -0.182    |
| [(GC),(TA)] | O <sub>6</sub> (G)         | -0.138                 | 0.104     | -0.127                  | 0.102     |
|             | N <sub>6</sub> (A)         | 0.167                  | -0.193    | 0.179                   | -0.202    |

<sup>a</sup> Letters in parentheses indicate the purine base to which a given atomic center belongs. <sup>b</sup> Calculations at the HF/6-31G\* level for donors and acceptors in resonance. Because of the double  $\zeta$  quality of the basis set, two sets of coefficients are displayed for each atomic center.

rationalize the increasing electronic coupling, 0.089 vs 0.122 eV (Table 2).

Complexes with interstrand purines are simpler to analyze because there are only few orbital "contacts". For instance, in [(GC),(TA)], there is an overlapping region between O<sub>6</sub> of guanine and N<sub>6</sub> of adenine (Figure 4). Both centers are involved in hydrogen bonds between purines and pyrimidines: O<sub>6</sub>(G) acts as proton acceptor, while N<sub>6</sub>(A) acts as a proton donor. Therefore, the hydrogen bonds are expected to exert opposing charge donation effects and it is difficult to predict the total change on the coupling. Inspection of Figure 4 suggests that the contribution of N<sub>6</sub>(A) is more important. Indeed, the electronic coupling increases slightly, by 0.005 eV, when one goes from the simple purine model G:A (0.021 eV) to the WCP dimer [(GC),(TA)] (0.026 eV; Table 2). In the intrastrand case [(GC),(AT)] analyzed above, both hydrogen bonds work in the same direction and lead to a significant increase of the coupling, 0.033 eV. The LCAO coefficients listed in Table 4 confirm this qualitative type of reasoning for the interstrand example [(GC),(TA)]. When the WCP dimer is formed, the  $p_{\pi}$  coefficients associated with the proton donor N<sub>6</sub>(A) increases while the corresponding coefficients of the proton acceptor O<sub>6</sub>(G) decrease.

The importance of hydrogen bonding between nucleobases has been pointed out many times;<sup>52,53</sup> it plays a fundamental role in preserving the integrity of DNA. Here, we demonstrated the effect of hydrogen bonding within WCPs on the hole transfer through the  $\pi$ -stack of DNA. Note that hydrogen bonds between nucleobases originate from specific structural features of interacting monomers. Therefore, with the current set of models, it is not possible to isolate hydrogen-bond effects and to assess quantitatively the corresponding contributions to the variation of the electronic coupling. The analysis of MO representations can also be used profitably to rationalize changes of the electronic coupling when the relative geometry of a WCP dimer deviates from the ideal DNA structure.<sup>29,54</sup>

## Conclusions

A detailed analysis of the effects of pyrimidine nucleobases on the electronic coupling matrix elements of hole transfer in DNA has been carried out using WCP dimers as models. We considered 10 possible complexes and compared matrix elements calculated for the complexes and the corresponding purine dimers.

We were unable to identify any orbital-based direct involvement of the pyrimidine nucleobases in the hole transfer. Hole

transfer proceeds through purine bases independent of their intra or interstrand arrangement, but the electronic coupling is strongly affected by pyrimidine bases via electrostatic and exchange interaction between the nucleobases as well as by the formation of hydrogen bonds within the WCPs.

A charge partitioning analysis (CDA) demonstrated that the polarization of purines is remarkable when the pyrimidine bases are added in the formation of WCPs while HOMO and HOMO-1 of the purine dimers remain qualitatively unchanged.

The point charge model confirmed the importance of the polarization of the purines caused due to the pyrimidine bases. However, notable deviations of the electronic coupling predicted by these ESP models from the corresponding values determined with WCP dimers indicate an essential role of other interactions. A CSOV analysis revealed that the exchange interaction between purine and pyrimidine units plays a crucial role; it also shows that the polarization of the pyrimidines leads to small corrections of the electronic coupling between the purine moieties (usually below 10%).

An analysis of the spatial distribution of HOMO and HOMO-1 orbitals in WCP dimers (with the purine bases "in resonance") provided a qualitative understanding of the electronic coupling. Hydrogen bonding between purine and pyrimidine bases clearly affects the electronic coupling.

When describing charge migration along the  $\pi$ -stack of DNA, it seems most appropriate to discuss the electron coupling between WCPs as the smallest units. In other words, less accurate results emerge if one uses perturbation theory, treating pyrimidines as bridge sites, to improve the direct electronic coupling of adjacent purine bases.

**Acknowledgment.** We are grateful to D. Ganyushine, S. Krüger, A. Matveev, M. Süzen, and M. Sobczyk for valuable assistance. We thank Prof. G. Frenking for supplying the CDA package. J.R. acknowledges a fellowship of the Alexander von Humboldt Foundation. This work was supported by Deutsche Forschungsgemeinschaft, Volkswagen Foundation, and Fonds der Chemischen Industrie, Germany.

## References and Notes

- (1) Barbara, P. F.; Olson, E. J. *Adv. Chem. Phys.* **1999**, *107*, 647.
- (2) Schuster, G. B. *Acc. Chem. Res.* **2000**, *33*, 253.
- (3) Giese, B. *Acc. Chem. Res.* **2001**, *34*, 159.
- (4) Giese, B.; Spichty, M. *Chem. Phys. Chem.* **2000**, *1*, 195.
- (5) Lewis, F. D.; Letsinger, R. L.; Wasielewski, M. R. *Acc. Chem. Res.* **2001**, *34*, 159.
- (6) Newton, M. D. *Chem. Rev.* **1991**, *91*, 767.
- (7) Issue no. 3 of *Chem. Rev.* **1992**, *92*, 2.
- (8) Jortner, J.; Bixon, M., Eds. *Electron Transfer: From Isolated Molecules to Biomolecules*. *Adv. Chem. Phys.*; Wiley: New York, 1999; Vols. 106 and 107.
- (9) Armitage, B. *Chem. Rev.* **1998**, *98*, 117.
- (10) Barrows, C. J.; Muller, J. G. *Chem. Rev.* **1998**, *98*, 1109.
- (11) Kelley, S. O.; Jackson, N. M.; Hill, M. G.; Barton, J. K. *Angew. Chem., Int. Ed. Engl.* **1999**, *38*, 941.
- (12) Fox, M. A. *Acc. Chem. Res.* **1999**, *32*, 201.
- (13) Lisdorf, F.; Ge, B.; Scheller, F. W. *Electrochem. Commun.* **1999**, *1*, 65.
- (14) Netzel, T. L. In *Organic and Inorganic Photochemistry*; Ramamurthy, V., Schanze, K. S., Ed.; Marcel Dekker, Inc.: New York, 1998.
- (15) Jortner, J.; Bixon, M.; Langenbacher, T.; Michel-Beyerle, M.-E. *Proc. Nat. Acad. Sci. U.S.A.* **1998**, *95*, 12759.
- (16) Bixon, M.; Jortner, J. *J. Phys. Chem. B* **2000**, *104*, 3906.
- (17) Berlin, Yu. A.; Burin, A. L.; Ratner, M. A. *J. Phys. Chem. A* **2000**, *104*, 443.
- (18) Berlin, Yu. A.; Burin, A. L.; Ratner, M. A. *J. Am. Chem. Soc.* **2001**, *123*, 260.
- (19) Olofsson, J.; Larsson, S. *J. Phys. Chem. B* **2001**, *105*, 10398.
- (20) Steenken, S.; Jovanovic, S. C. *J. Am. Chem. Soc.* **1997**, *119*, 617.
- (21) Orlov, V. M.; Smirnov, A. N.; Varshavsky, Y. M. *Tetrahedron Lett.* **1976**, *48*, 4377.

- (22) Voityuk, A. A.; Jortner, J.; Bixon, M.; Rösch, N. *Chem. Phys. Lett.* **2000**, *324*, 430.
- (23) Marcus, R. A.; Sutin, N. *Biochim Biophys. Acta* **1982**, *811*, 265.
- (24) Mikkelsen, K. V.; Ratner, M. A. *Chem. Rev.* **1997**, *87*, 1113.
- (25) Larsson, S. *J. Am. Chem. Soc.* **1981**, *103*, 4034.
- (26) Skourtis, S. S.; Beratan, D. N. *Adv. Chem. Phys.* **1999**, *106*, 377.
- (27) Priyadarshy, S.; Risser, S. M.; Bertan, D. N. *J. Phys. Chem.* **1996**, *100*, 17678.
- (28) Voityuk, A. A.; Rösch, N. *J. Phys. Chem. B* **2002**, *106*, 3013.
- (29) Voityuk, A. A.; Siri Wong, K.; Rösch, N. *Phys. Chem. Chem. Phys.* **2001**, *3*, 5421.
- (30) Saito, I.; Takayama, M.; Sugiyama, H.; Nakatani, K.; Tsuchida, A.; Yamamoto, M. *J. Am. Soc. Chem.* **1995**, *117*, 6406.
- (31) Saito, I.; Nakamura, T.; Nakatani, K.; Yoshioka, Y.; Yamaguchi, K.; Sugiyama, H. *J. Am. Chem. Soc.* **1998**, *120*, 12686.
- (32) Voityuk, A. A.; Rösch, N.; Bixon, M.; Jortner, J. *J. Phys. Chem. B* **2000**, *104*, 9740.
- (33) Voityuk, A. A.; Jortner, J.; Bixon, M.; Rösch, N. *J. Chem. Phys.* **2001**, *114*, 5614.
- (34) Rodriguez-Monge, L.; Larsson S. *J. Phys. Chem.* **1996**, *100*, 6298.
- (35) Bagus, P. S.; Herman, K.; Bauschlicher, C. W., Jr. *J. Chem. Phys.* **1984**, *80*, 4378.
- (36) Bagus, P. S.; Herman, K.; Bauschlicher, C. W., Jr. *J. Chem. Phys.* **1984**, *81*, 1966.
- (37) Bagus, P. S.; Illas, F. *J. Chem. Phys.* **1992**, *96*, 8962.
- (38) Lu, X. J.; El Hassan, M. A.; Hunter, C. A. *J. Mol. Biol.* **1997**, *273*, 681.
- (39) Katz, D. J.; Stuchebrukhov, A. A. *J. Chem. Phys.* **1997**, *106*, 5658.
- (40) Cave R. J.; Newton, J. *Chem. Phys.* **1997**, *106*, 9213.
- (41) Cave R. J.; Newton, J. *Chem. Phys. Lett.* **1996**, *249*, 15.
- (42) Hariharan, P. C.; Pople, J. A. *Theor. Chim. Acta* **1973**, *28*, 213.
- (43) Besler, B. H.; Merz, Jr., K. M.; Kollman, P. A. *J. Comput. Chem.* **1990**, *11*, 431.
- (44) Singh, U. C.; Kollman, P. A. *J. Comput. Chem.* **1984**, *5*, 129.
- (45) Dapprich, S.; Frenking, G. *J. Phys. Chem.* **1995**, *99*, 9352.
- (46) Dapprich, S.; Frenking, G. *CDA*, version 2.1; Philips-Universität Marburg, 1995.
- (47) Dupuis, M.; Marquez, A.; Davidson, E. R. HONDO 99.6, 1999; based on HONDO 95.3, Dupuis, M.; Marquez, A.; Davidson, E. R. Quantum Chemistry Program Exchange: Indiana University, Bloomington, IN 47405.
- (48) Frisch, M. J.; Trucks, G. W.; Schlegel, H. B.; Scuseria, G. E.; Robb, M. A.; Cheeseman, J. R.; Zakrzewski, V. G.; Montgomery, J. A., Jr.; Stratmann, R. E.; Burant, J. C.; Dapprich, S.; Millam, J. M.; Daniels, A. D.; Kudin, K. N.; Strain, M. C.; Farkas, O.; Tomasi, J.; Barone, V.; Cossi, M.; Cammi, R.; Mennucci, B.; Pomelli, C.; Adamo, C.; Clifford, S.; Ochterski, J.; Petersson, G. A.; Ayala, P. Y.; Cui, Q.; Morokuma, K.; Malick, D. K.; Rabuck, A. D.; Raghavachari, K.; Foresman, J. B.; Cioslowski, J.; Ortiz, J. V.; Stefanov, B. B.; Liu, G.; Liashenko, A.; Piskorz, P.; Komaromi, I.; Gomperts, R.; Martin, R. L.; Fox, D. J.; Keith, T.; Al-Laham, M. A.; Peng, C. Y.; Nanayakkara, A.; Gonzalez, C.; Challacombe, M.; Gill, P. M. W.; Johnson, B. G.; Chen, W.; Wong, M. W.; Andres, J. L.; Head-Gordon, M.; Replogle, E. S.; Pople, J. A. *Gaussian 98*, version A7; Gaussian, Inc.: Pittsburgh, PA, 1998.
- (49) Schaftenaar, G.; Noordik, J. H. *J. Comput.-Aided Mol. Design* **2000**, *14*, 123.
- (50) Chęłasiński, G.; Szczeniński, M. *Chem. Rev.* **1994**, *94*, 1723.
- (51) Scheiner, S. *Hydrogen Bonding. A Theoretical Perspective*; Oxford University Press: New York, 1997.
- (52) Desfrancois, C.; Carles, S.; Schermann, J. P. *Chem. Rev.* **2000**, *100*, 3943.
- (53) Hobza, P.; Šponer, J. *Chem. Rev.* **1999**, *99*, 3247.
- (54) Voityuk, A. A.; Rak, J.; Siri Wong, K.; Rösch, N. To be published.